NUMERICAL ANALYSIS OF DRYING SCHEDULES OF REFRACTORY CASTABLES BY USING COMPUTING SIMULATIONS

T.M. Cunha(1)*, M.H. Moreira(1), M.F. Santos(1), R. A. Angélico(2), V.C. Pandolfelli(1)

(1) Federal University of Sao Carlos, Graduate Program in Materials Science and Engineering, São Carlos, SP, Brazil.

(2) University of São Paulo (USP), Department of Aeronautical Engineering, Av. Trabalhador São-Carlense, 400, São Carlos, Brazil.

*tulio@dema.ufscar.br

ABSTRACT

Refractory castables are broadly used as industrial equipment lining because of its thermal and mechanical properties at high temperature. For its processing, dry powder is mixed with water, which must be withdrawn via a controlled heating schedule, otherwise high pressure will build-up within the material might lead to explosive spalling. By using numerical simulations, this work aims to investigate the heating-up profiles displaying one plateau while varying the heating rate, holding time and its temperature. Plateaus held at 150°C were not as beneficial as just an increase of 30°C (180°C) on the temperature yielded a faster, yet safe, drying. A unique plateau at 350°C also might not be useful to the drying as pressure can reach its maximum value before the holding time. Increasing the wall thickness showed that these simple heating schedules are not suitable and longer dwell time or complex heating profiles might be required for its safe drying. Finally, computing the total energy consumption for each profile allows the end-user to develop a ranking system in order to choose the best heating schedule for their application.

INTRODUCTION

Refractory ceramics are present in the lining of equipment that operate at high temperatures as they provide both,- thermal insulation and/or high thermo-mechanical stability, allowing the production of diversified materials, as metal alloys and glasses [1].

Usually, they are split in two different groups: the shaped and the non-shaped. The first one is purchased in a definite geometry, whereas the latter is prepared in-situ and reaches the final shape at the application stage. The processing of these monolithic linings comprises, firstly,

Data citation: Proceeding title and author names available in the first page;

Source: Proceeding 11, XLII ALAFAR Congress, Foz do Iguaçú, Brazil, 2022

the mix of the ceramic powder with water and additives, then they are cast on the equipments' walls or bottom, followed by a controlled heating schedule [2,3]. The reason for this lies on the intrinsic moisture contained within the pores, which is needed for the action of the binder and also for the easiness of homogenization [3].

If heated too quickly, the moisture will try to be released in a higher rate than the microstructure allows the water vapor to escape it, resulting in a pressure build-up that, combined with thermomechanical stress due to the thermal gradient, can result in an explosive spalling, damaging both the lining and possibly the equipment, affecting the operation safety [3,4].

The heating schedule commonly applied by various industry sectors always include heating ramps and holding times, with time lengths directly related to the thickness of the monolithic layer. Nevertheless, there is no consensus about the heating rate to be applied, or even in which temperature or how long the heating should be held [4].

Thus, this work tries to evaluate the effect of different routes on the heating schedule design, presenting a comparison between the generated pressure, the local mechanical strength of the material and also the amount of energy consumed during the process. Lastly, a novel methodology for profile selection is proposed, based on aspects related to the pressure levels, energy consumption and drying state.

MATERIALS AND METHODS

Material and properties

The material used as a reference is a high alumina cement bonded castable composition, referred as 5CAC for containing 5% of the weight of calcium aluminate cement. Table 1 displays the raw materials, their fractions and suppliers of such composition [5].

Table 1: Composition of 5CAC castable

Raw Material	Mass Fraction (%)	Supplier
Tabular Alumina (<5mm)	74	T-60, Almatis, Germany
Calcinated Alumina	11	CL370, Almatis, Germany
Reactive Alumina	10	CT30000SG, Almatis, Germany
CAC	5	Secar 71, Imerys Aluminates, France
Dispersant	0.2	Castament FS60, BASF, Germany
Distilled Water	4.5	-

The castable was designed to fit an Andreassen particle distribution with coefficient of 0.21. The raw materials were homogenized with water and dispersant in a home-made rheometer [6] and then the composition was shaped as 50 mm height x 50 mm diameter cylinders for the thermogravimetric analyses, 25 mm x 25 mm x 150 mm bars for three points bending tests, 233 mm x 114 mm x 64 mm bricks for the measurement of thermal conductivity and 22 mm height x 38.2 mm diameter cylinders for evaluating the permeability. All of them were cured at 30°C for 24 hours at 90% relative humidity and all samples but the TGA ones were pre-fired in temperatures ranging from 300°C to 500°C for 5 hours.

The thermal conductivity and heat capacity were measured via the hot wire method, ISO 8894-2, the permeability at room temperature followed ASTM C577, the density was obtained via the Archimedes' method (ASTM C830-00), and the mechanical strength was carried out under three points bending tests (ASTM C583-15) at a loading rate of 12.9 N/s in a MTS 810 USA.

It is shown in Figure 1 the variation of the thermal conductivity with temperature, with both measured values and a fitting curve for them, which was used for the computing simulation. Figure 2 displays an extrapolation of a dynamic permeability based on the measured value at room temperate for the pre-dried sample and the hot air flow rate measurements attained by Ribeiro et al. [7, 8]. This procedure is thoroughly described in [5].

Figure 1: a) Thermal conductivity for 5CAC castable. b) Dynamic permeability obtained were based on the measured value and hot air flow rate data by Ribeiro et al. [8].

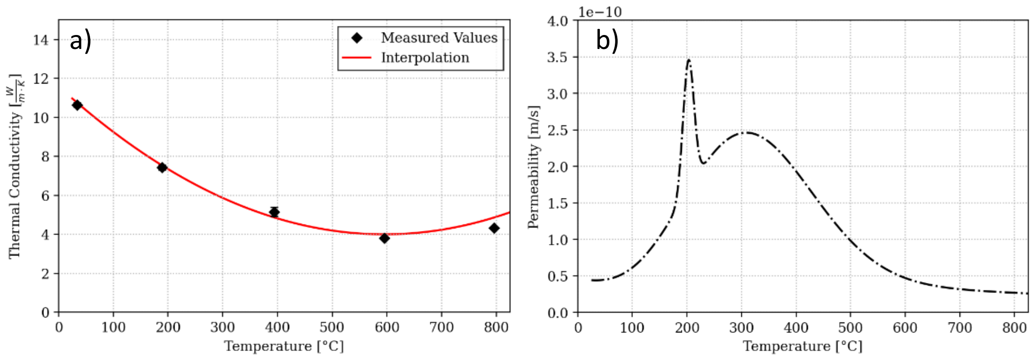

To compare the pressure that was built-up inside the material microstructure with the local mechanical strength, a novel parameter was used [5], named resistance ratio, which is a ratio between the local vapor pressure and the local triaxial mechanical strength. To obtain the latter, the three-point bending strength value was converted into uniaxial tensile strength considering Weibull modulus (m = 10.1, measured after curing for 24 h at 30°C and drying at 110°C for 24 h), which was then changed to a triaxial resistance with the help of Hooke's law, assuming Poisson ratio of 0.15. Figure 2 shows the obtained values as well as each conversion step, followed by the fitting curve obtained to be used for the computing model.

Figure 2: Conversion steps from three-point bending test to triaxial tensile strength.

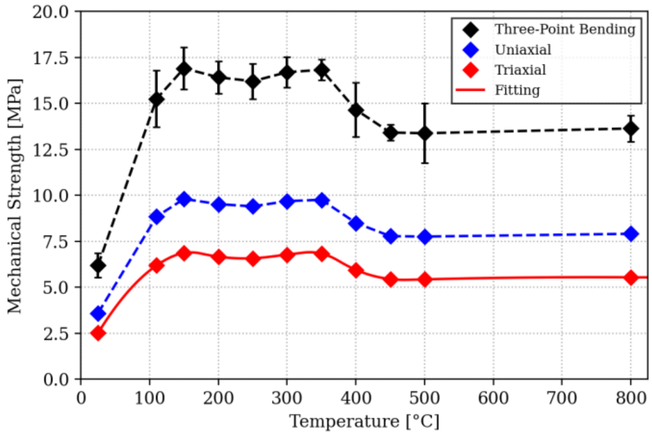

Simulation Setup

The numerical model considered the transport of a single phase which represents both the water vapor and liquid water within the material and it was described on a former publication by the research group [9], being based on the works by Bazant [10] and Gong [11].

Regarding the simulation parameters, it was defined that the heating schedule would start at 25°C and finish at 925°C, applying heating rates of 50°C/h, 75°C/h or 100°C/h during the non-holding periods. These plateaus of temperature were set to last for 30 hours, so the variation of moisture within the material can be observed. The geometry used was a unidimensional mesh, based on the complex configuration of a steel ladle [12], comprising (I) the working layer, (II) the permanent layer, (III), the insulating one and (IV) the metallic shell.

This geometry is shown in Figure 3, whereas the properties of each individual layer can be found in [5]. The thickness of the layer I is either 10, 20 or 30 cm.

The boundary conditions applied were: (i) imposed heating schedule on the hot face of the layer I, whereas the cold side of layer IV undergoes a cooling process via radiation and convection. Because the drying process occurs only for layer I, it was considered both hot face and the interface with layer 2 as permeable, with the latter being justified by the porosity of layer II material and the non-perfect coupling of the layers. Lastly, at the initial stage of each simulation, all the elements were set for 25°C and 2850 Pa as partial vapor pressure.

The energy computation was also carried out during the simulation time, with the values of the different heat fluxes being extracted on every element and computed in a post-processing algorithm. This process was triple checked via different methodologies to assess that the attained value is the total consumed energy for each simulation set.

Figure 3: Geometry used, adapted from the work by Santos et al. [12]

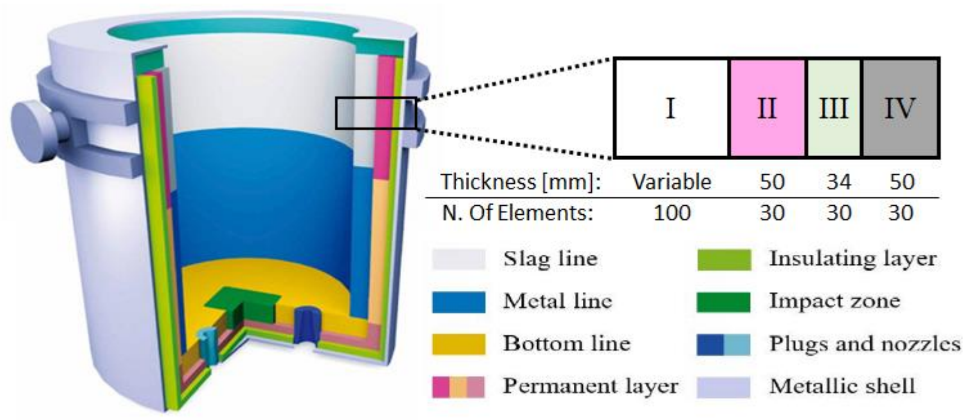

RESULTS

Firstly, the simulations were carried out and the results analyzed. Figures 4 to 7 show the profile of the maximum pressure over time; the water content sources; whether free adsorbed water and/or chemically bound water; as well as the thermal profile comparing the hot and cold faces of the monolithic layer for the heating rate of 50°C/h. The results for the 30 cm thick lining will not be displayed here as not a single simulation resulted in a complete drying of it, even after 40 hours of a total heating profile.

Figure 4: Profiles of temperature, water content and temperature obtained for the lining with 10cm of thickness of 5CAC at a heating rate of 50°C/h for the non-holding periods.

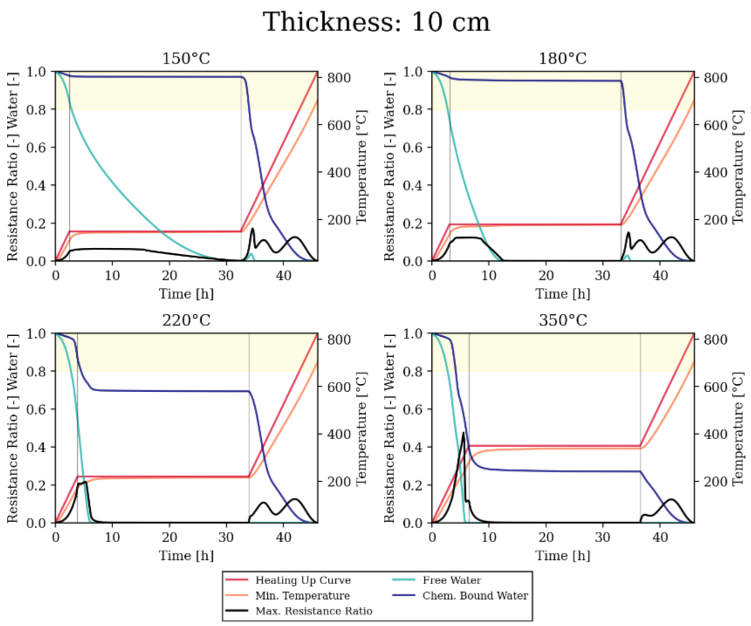

Figure 5: Profiles of temperature, water content and temperature obtained for the lining with 20cm of thickness of 5CAC at a heating rate of 50°C/h for the non-holding periods.

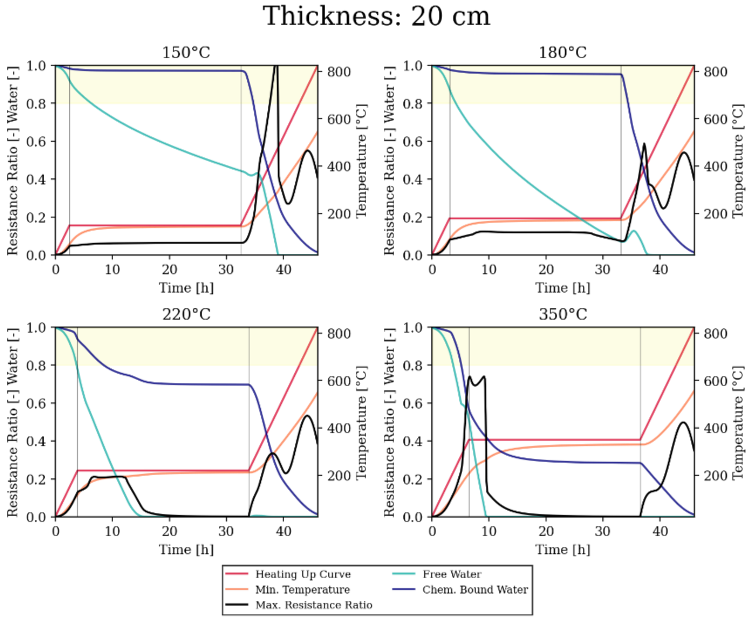

Regardless of the temperature plateau, there was no risk of explosion as the values of resistance ratio in Figures 4 and 5 were far under 1.0, which indicates safeness of drying, even though the profiles were not optimized. Another important point that can be observed is that an unique plateau at 150°C was shown to be inefficient when compared to that at 180°C, as the lower temperature slows the withdrawal of the free adsorbed water, resulting in similar pressure scenarios to those at 180°C for a thickness of 10 cm. The higher risk for explosion in a thickness of 20 cm, Figure 5, can be attributed due to the fact that below ~220°C the chemically bounded water is almost not removed, while the drying process of adsorbed water can still occur, as it is not only a function of temperature, but also of the relative humidity. At higher temperatures, the pressure was virtually the same for all scenarios as the only source of water at that moment is the chemically bounded one.

At a higher heating rate, as 100°C/h, shown in Figures 6 and 7, the inefficiency of the holding period at 150°C can still be observed, yet not only that, but also high values of resistance ratio start to show up for a thickness of 20 cm. The reason of this behavior is that the free water was not dried entirely during the first plateau, and the remaining quantity was withdrawn alongside the chemically bonded water, resulting in peak pressures. This is an indicative that a likely strategy for optimization of the drying could be the total split of these two different sources: a first temperature plateau at a temperature under the hydrate decomposition one and another shorter one above it, as the pressure peaks appear to not achieve high enough values to justify longer holding periods.

Figure 6: Profiles of temperature, water content and temperature obtained for the lining with 10cm of thickness of 5CAC at a heating rate of 100°C/h for the non-holding periods.

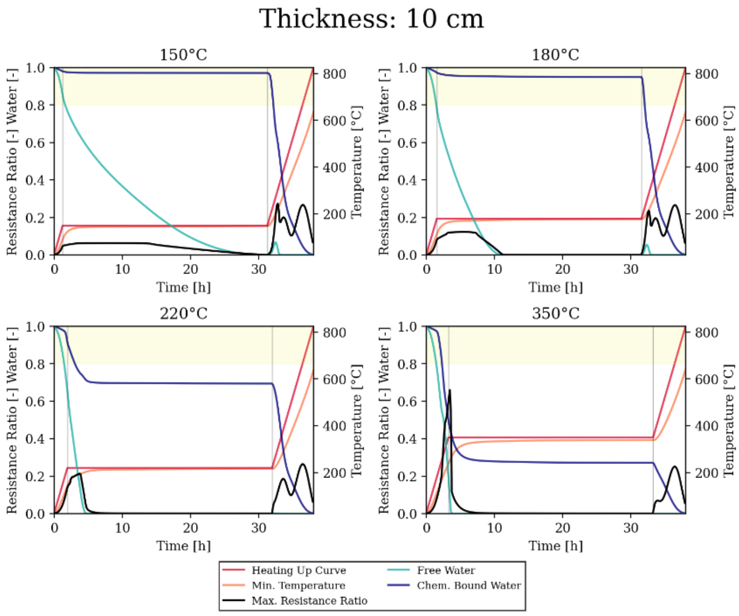

Figure 7: Profiles of temperature, water content and temperature obtained for the lining with 20cm of thickness of 5CAC at a heating rate of 100°C/h for the non-holding periods.

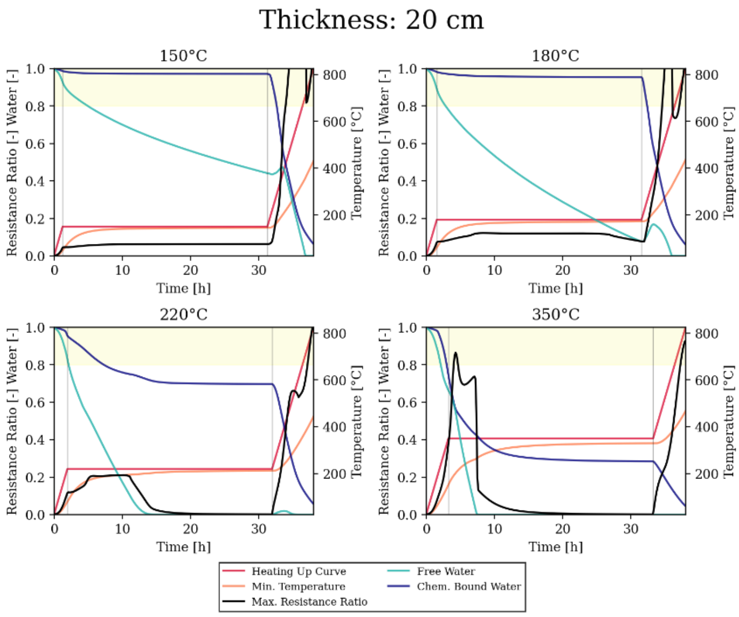

Lastly, the energy was computed following the method described and, based on it, a novel ranking methodology is proposed, considering the drying profile, the resistance ratio and the energy consumption.

Comparing all simulations runs and the amount of water remaining for both sources at the very last time step, many of them still presented significative water contents that indicated an incomplete drying process. So, in order to assess which were successful by these criteria, it was established that any simulation resulting in 5 wt% of the initial water content or below it would be considered dried, and therefore allowed to be picked as viable for application. Figure 8 displays the quantity of water remaining for every simulation carried out.

The second comparison was based on whether each result reached a resistance ratio close to a safety factor of 0.8, as values above this number are considered risky. Figure 9 shows all values obtained and the selected profiles are highlighted with a green checkmark.

Figure 8: Chemically bounded and free water content at the last simulation step. All simulations are displayed and plotted according to the residual water, normalized at 1, at the last timestep. π indicates the plateau temperature.

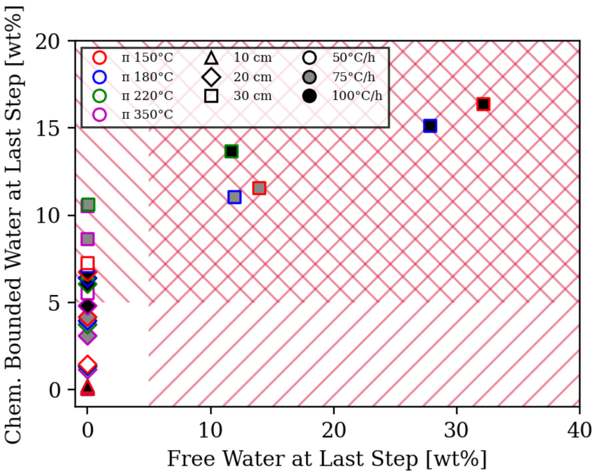

Figure 9: All remaining simulations are displayed and presented in an ascending order of resistance ratio value. Those with a value higher than 0.8 were disregarded.

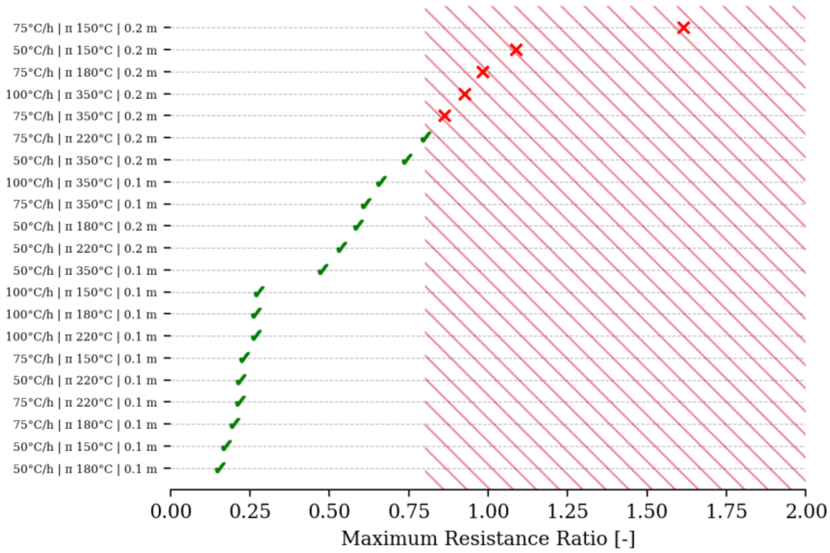

Finally, the energy consumption was used to rank the remaining profiles, ranking from the most economic to the most expensive energy-wise ones as shown in Figure 10. Based on this, it was possible to assess that, among all the simulations carried out, not a single profile would be fit for a 30 cm thickness layer. Profiles considering 75°C/h for π=350°C and 50°C/h for π=180°C would be the best ones for a 20 cm thickness, whereas 100°C/h for π=180°C and 100°C/h for π=150°C, would be the preferred ones for 10 cm thickness, assuming a fixed total heating time for all scenarios.

Figure 10: Last step of the methodology, all remaining simulations were ranked based on the total consumed energy.

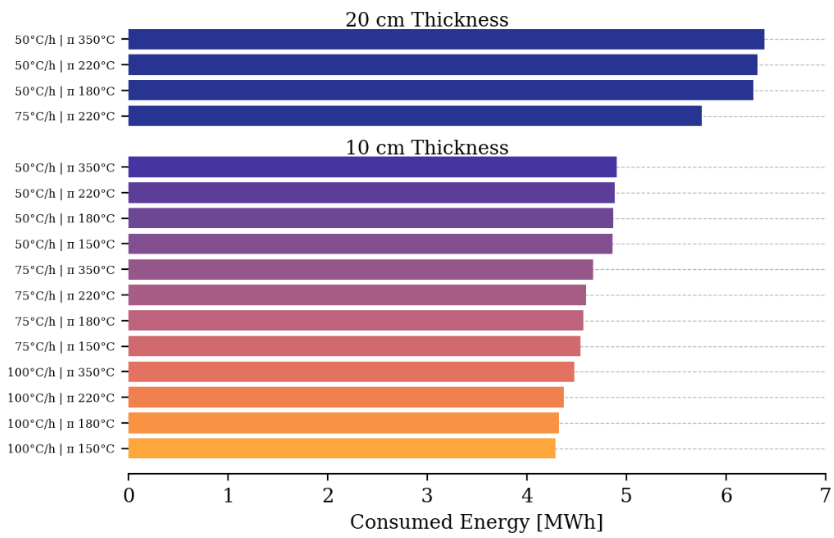

CONCLUSIONS

This work presented an original methodology to select the heating schedule which led to the following suggestions: i) plateaus at temperatures much lower than the dehydration ones might not be much beneficial, ii) larger thicknesses might require either longer holding periods or more complex schedules, iii) a likelihood of achieving a safe drying would present plateaus for the withdrawal of free water and for chemically bonded on, and iv) the computation of consumed energy allows the end-user to develop a robust curve selection tool to pick the most suitable one based on the design target. Although some of the conclusions are already carried out by the refractory community, this match between the numerical simulation and the usual practice, provides confidence that novel heating schedules can be analysed and proposed, fulfilling the aimed target of less CO_2 generation and energy saving.

AKNOWLEDGEMENTS

This study was financed in part by the Coordenação de Aperfeiçoamento de Pessoal de Nível Superior - Brasil (CAPES) - Finance Code 001. The authors would like to thank the Conselho

Nacional de Desenvolvimento Cientifico e Tecnologica – CNPq (grant number: 134347/2019-6) and Fundação de Amparo à Pesquisa do Estado de São Paulo - FAPESP (grant number: 2021/00251-0) for supporting this work. Finally, the authors are thankful for the support of F.I.R.E. and to A. P. da Luz for the experimental assistance at the early steps of this research.

REFERENCES

[1] C. Schacht, Refractories Handbook, CRC Press, Hoboken, 2004. OCLC: 910581448.

[2] W. Lee, W. Vieira, S. Zhang, K. Ahari, H. Sarpoolaky, C. Parr, Castable refractory concretes, International Materials Reviews 46 (2001) 145–167.

[3] A. P. Da Luz, M. d. A. L. Bráulio, V. C. Pandolfelli, Refractory Castable Engineering, 2015.

[4] M. Moreira, S. Pont, R. Ausas, A. Luz, T. Cunha, C. Parr, V. Pandolfelli, Main trends on the simulation of the drying of refractory castables - review, Ceramics International 47 (2021) 28086–28105.

[5] T. Cunha, M. Moreira, M. Santos, A. Luz, V. Pandolfelli, Drying behavior of steel-ladle lining refractory castables under continuous heating rate, Ceramics International 48 (2022) 1142–1151.

[6] R. Pileggi, V. Pandolfelli, A. Paiva, J. Gallo, Novel rheometer for refractory castables, American Ceramic Society Bulletin 79 (2000) 54–58.

[7] C. R. Oliveira, Effects of temperature and drying additives in the permeability of refractory castables, 2002. Dissertation , PPG-CEM UFSCar, São Carlos, Brazil. (In Portuguese).

[8] C. Ribeiro, M. Innocentini, V. C. Pandolfelli, Dynamic permeability behavior during drying of refractory castables based on calcium-free alumina binders, Journal of the American Ceramic Society 84 (2004) 248 – 250.

[9] M. Moreira, A. Luz, T. M. Cunha, H. Lemaistre, J. Auvray, C. Parr, R. F. Ausas, V. Pandolfelli, Practical numerical simulation and experimental setup for speeding up the drying behavior of calcium aluminate cement (CAC)-bonded refractory castables, in: UNITECR'19. Proc. Unified Int. Tech. Conf. on Refractories. 16th Biennial Worldwide Congress. "Refractories For the Future", volume 1, 2019, pp. 167–169.

[10] Z. P. Bažant, W. Thonguthai, Pore pressure in heated concrete walls: theoretical prediction, Magazine of Concrete Research 31 (1979) 67–76.

[11] Z.-X. Gong, A. S. Mujumdar, A model for kiln-drying of refractory concrete slabs, Drying Technology 11 (1993) 1617–1639.

[12] M. Santos, M. Moreira, M. Campos, P. I. Pelissari, R. Angélico, E. Sako, S. Sinnema, V. C. Pandolfelli, Enhanced numerical tool to evaluate steel ladle thermal losses, Ceramics International 44 (2018) 12831-12840.